

1 **Comparison of linear combination modeling strategies for GABA-edited MRS**
2 **at 3T**

3 Helge J. Zöllner^{1,2}, Sofie Tapper^{1,2}, Steve C. N. Hui^{1,2}, Peter B. Barker^{1,2}, Richard A. E. Edden^{1,2},
4 Georg Oeltzschner^{1,2,*}

5 ¹ *Russell H. Morgan Department of Radiology and Radiological Science, The Johns Hopkins*
6 *University School of Medicine, Baltimore, MD, United States*

7 ² *F. M. Kirby Research Center for Functional Brain Imaging, Kennedy Krieger Institute, Balti-*
8 *more, MD, United States*

9

10 ***Corresponding author:**

11 Georg Oeltzschner, Ph.D.

12 Division of Neuroradiology, Park 367G

13 The Johns Hopkins University School of Medicine

14 600 N Wolfe St

15 Baltimore, MD 21287

16 goeltzsl@jhmi.edu

17

18

19 *Running title: Linear combination modeling of GABA-edited MRS*

20 *Word count: 5992*

21 **Keywords**

- 22 • Magnetic resonance spectroscopy
- 23 • Linear combination modeling
- 24 • GABA-edited MEGA-PRESS

25 Abstract

26 Purpose

27 J-difference-edited spectroscopy is a valuable approach for the in vivo detection of γ -aminobu-
28 tyric-acid (GABA) with MRS. A recent expert consensus article recommends linear combination
29 modeling (LCM) of edited MRS, but does not give specific details of implementation. This
30 study explores different modeling strategies to adapt LCM for GABA-edited MRS.

31 Methods

32 62 medial parietal lobe GABA-edited MEGA-PRESS spectra from a recent 3T multi-site study
33 were modeled using 102 different strategies combining six different approaches to account for
34 co-edited macromolecules, three modeling ranges, three baseline knot spacings, and using basis
35 sets with or without homocarnosine. The resulting GABA and GABA+ estimates (quantified rel-
36 ative to total creatine), the residuals at different ranges, SDs and CVs, and Akaike information
37 criteria, were used to evaluate the models' performance.

38 Results

39 Significantly different GABA+ and GABA estimates were found when a well-parameterized
40 MM_{3co} basis function was included in the model. The mean GABA estimates were significantly
41 lower when modeling MM, while the CVs were similar. A sparser spline knot spacing led to
42 lower variation in the GABA and GABA+ estimates and a narrower modeling range – only in-
43 cluding the signals of interest – did not substantially improve or degrade modeling performance.
44 Additionally, results suggest that LCM can separate GABA and the underlying co-edited MM_{3co}.
45 Incorporating homocarnosine into the modeling did not significantly improve variance in
46 GABA+ estimates.

48 Conclusion

49 GABA-edited MRS is best quantified by LCM with a well-parameterized co-edited MM_{3co} basis
50 function with a constraint to the non-overlapped MM_{0,93} in combination with a sparse spline knot
51 spacing and a modeling range between 0.5 and 4 ppm.

52 Introduction

53 A recent expert consensus paper recommended that linear combination modeling (LCM) should
54 be used for the quantification of edited MRS data¹, stating that standard fitting approaches origi-
55 nally optimized for short-TE MRS should be adapted for edited MRS. Further, it was recom-
56 mended that quantum-mechanical simulations should be used to confirm the co-edited profile of
57 all metabolites in the edited spectrum, and contributions from macromolecule (MM) signals
58 should be specified. Despite these recommendations, little detail was given regarding several
59 unique features of edited spectra, and how they should be appropriately modeled. These features
60 include:

- 61
62 1) The MEGA-PRESS experiment is well-known to co-edit MM signals with coupled spins
63 at 1.7 and 3 ppm, causing substantial contamination of the edited GABA signal, and
64 forcing researchers to report the composite measure GABA+MM (GABA+)¹. Because
65 the co-edited MM signal is poorly characterized, there is currently no consensus or
66 recommendation on how to appropriately account for it during spectral modeling.
67 Instead, the most widely used analysis algorithms implement entirely different strategies
68 to fit the composite 3-ppm signal. For example, the Gannet software uses a single
69 Gaussian model², while a double-Gaussian is used in Tarquin³, and LCModel⁴ defaults to
70 a basis set that only includes the GABA basis function.
- 71 2) Another co-edited compound contributing to the 3 ppm signal is homocarnosine (HCar),
72 a dipeptide of GABA and histidine. While the 3 ppm multiplets of GABA and
73 homocarnosine are separated by just 0.05 ppm (which are therefore unlikely to be
74 successfully separated), inclusion of a homocarnosine basis function may be warranted
75 based on its reported concentration in vivo (~0.5 mmol/kg⁵, compared to ~1-2 mmol/kg
76 for GABA), but it has not been investigated whether doing so has a stabilizing or
77 destabilizing effect on the modeling⁶.
- 78 3) Unedited spectra are typically modeled over a restricted frequency-domain range
79 covering the visible upfield peaks, including macromolecular and lipid resonances
80 between 0 and 1 ppm, but usually avoiding the water suppression window above ~4 ppm.
81 The choice of frequency-domain modeling range for edited spectra is less obvious. Since

82 the main advantage of spectral editing is the isolation of a single target resonance,
83 modeling signals outside the immediate surrounding of the target may dilute the resolving
84 power of editing. On the other hand, increasing the modeling range may offer useful
85 constraints to stabilize the solution of the modeling problem. The difference is
86 highlighted by the different strategies encountered in common software tools – while the
87 Gannet software fits the GABA-edited difference spectrum over a narrow range (only
88 including the 3-ppm GABA+ and 3.75 ppm glutamate and glutamine peaks), the
89 LCMModel recommendation is to include the strong co-edited signals from glutamate
90 (Glu), glutamine (Gln), glutathione (GSH), N-acetylaspartylglutamate (NAAG), N-
91 acetylaspartate (NAA), which heavily overlap with GABA around 2.25 ppm. The effects
92 of limiting the modeling range have not been assessed systematically to date.

93 4) Linear combination modeling methods commonly include terms to account for smooth
94 baseline curvature, usually parametrized from cubic B-spline or polynomial functions, or
95 by smoothing residuals. The flexibility of the baseline model substantially affects
96 metabolite estimates from unedited spectra⁷; while baseline terms are necessary to
97 account for e.g. lipid contamination, poor water suppression etc., they are potential
98 sources of overfitting if awarded too many degrees of freedom. Baseline modeling may
99 have an even greater influence when modeling difference spectra, since only *co-edited*
100 lipid and MM signals contribute to the smooth background variation. Importantly, the co-
101 edited MM background of the GABA-edited difference spectrum has not been
102 appropriately characterized (e.g., through metabolite-nulled acquisition), suggesting that
103 the choice of baseline flexibility can drastically influence modeling results through two
104 highly susceptible regions of the spectrum. First, in the absence of an appropriate model
105 for the co-edited broad MM signal at 3 ppm, this signal may be absorbed into the baseline
106 depending on its flexibility. Second, strong MM and lipid signals in the region between
107 0.5 and 2.5 ppm may be affected by the 1.9 ppm editing pulse (either directly through
108 saturation or indirectly through coupling), likely leading to an unknown, but substantial,
109 MM contribution in this spectral region^{8,9}. This is especially important considering that
110 the co-edited signals from NAA, NAAG, Glu, Gln, and GSH overlap with GABA in this
111 region. Overly rigid baselines may provide insufficient flexibility to capture these signals,
112 in turn compromising the accuracy of the estimation of the co-edited metabolites.

113 The aim of this study was to evaluate different strategies for linear combination modeling of
114 GABA-edited MEGA-PRESS difference spectra, and to establish initial ‘best practices’ substan-
115 tiating the recommendations of the expert consensus on spectral editing. To this end, different
116 approaches to account for co-edited MM signals, various modeling ranges and baseline knot
117 spacings, as well as the inclusion of homocarnosine were compared. In the absence of a ‘gold
118 standard’, the performance of each modeling strategy was assessed by comparing descriptive sta-
119 tistics of the metabolite estimates, calculating the Akaike information criteria, and assessing the
120 fit residuals.

121 **Methods**

122 Study participants & data acquisition

123 In this study, 62 publicly available GABA-edited MEGA-PRESS datasets originating from 7
124 sites from a recent 3T multi-center study¹⁰ were analyzed (see **Supplementary Material 1** for
125 subject list). All datasets were acquired on Philips 3T scanners with the following acquisition pa-
126 rameters: TR/TE = 2000/68 ms; 320 excitations (10m 40s scan time); 2 kHz spectral width; 2000
127 samples; 27-ml cubic voxel volume in the medial parietal lobe. For the edit-ON transients, the
128 editing pulses with 15 ms pulse duration and 82.5 Hz inversion bandwidth (FHWM) were ap-
129 plied at a frequency of 1.9 ppm to refocus the coupling evolution of the GABA spin system. For
130 the edit-OFF transients, the editing pulses were applied at a frequency of 7.5 ppm. Edit-ON and
131 edit-OFF transients were acquired in alternating order. An additional water reference scan was
132 acquired for each dataset using interleaved water referencing¹¹, i.e. one excitation with water
133 suppression and editing pulses deactivated every 40 water-suppressed excitations (total of 8 aver-
134 ages).

135

136 Data pre-processing

137 Data were analyzed in MATLAB using Osprey^{12,13}, a recently published open-source MRS anal-
138 ysis toolbox. Raw data were eddy-current-corrected¹⁴ based on the water reference, and individ-
139 ual transients were aligned separately within the edit-ON and edit-OFF conditions using the ro-
140 bust spectral registration algorithm¹⁵. Averaged edit-ON and edit-OFF spectra were aligned by
141 optimizing relative frequency and phase such that the water signal in the difference spectrum was
142 minimized. The final difference spectra for quantification were generated by subtracting the edit-
143 OFF from the edit-ON spectra. Finally, any residual water signal was removed with a Hankel
144 singular value decomposition (HSVD) filter¹⁶.

145

146 Basis set

147 The basis set used for modeling was generated from a fully localized 2D density-matrix simula-
148 tion implemented in a MATLAB based simulation toolbox FID-A¹⁷, using vendor-specific refo-
149 cusing pulse shape and duration, sequence timings, and phase cycling. It contains 17 metabolite
150 basis functions (ascorbate, aspartate, creatine (Cr), negative creatine methylene (-CrCH₂),

151 GABA, glycerophosphocholine, GSH, Gln, Glu, water, myo-inositol, lactate, NAA, NAAG,
152 phosphocholine, phosphocreatine (PCr), phosphoethanolamine, scyllo-inositol, and taurine) and
153 8 Gaussian MM and lipid resonances (MM_{0.94}, MM_{1.22}, MM_{1.43}, MM_{1.70}, MM_{2.05}, Lip09, Lip13,
154 Lip20, defined as described in the LCModel software manual¹⁸) for the edit-OFF spectrum.

155
156 For the difference spectrum, MM_{0.94} and the co-edited macromolecular signal at 3 ppm (MM_{3co})
157 were parametrized as Gaussian basis functions (MM_{0.94}: 3-proton signal; chemical shift 0.915
158 ppm, full-width at half-maximum (FWHM) 11 Hz; MM_{3co}: 2-proton signal; chemical shift 3
159 ppm; FWHM 14 Hz). The MM_{0.94} amplitude was defined as described in the LCModel software
160 manual. The MM_{3co} amplitude was defined under the assumption of a pseudo-doublet GABA
161 signal at 3 ppm and the MM_{3co} contribution to the 3-ppm GABA peak to be around 50%^{1,6,8,19}.
162 The optimum FWHM used to parametrize the MM_{3co} basis function was determined to be 14 Hz
163 by fitting the mean difference spectrum of all datasets with a composite GABA+ basis function
164 (GABA + MM_{3co}) with varying FWHM (between 1 and 20 Hz). The parameterized Gaussian
165 MM_{3co} basis function was integrated into the modeling process using different assumptions and
166 constraints described in the following paragraphs.

167

168 Linear combination modeling of GABA-edited difference spectra

169
170 Osprey's frequency-domain linear combination model was used to determine the metabolite esti-
171 mates. Model parameters include metabolite basis function amplitudes, frequency shifts,
172 zero/first order phase correction, Gaussian and Lorentzian linebroadening, and cubic spline base-
173 line coefficients. All parameters are determined by Levenberg-Marquardt^{20,21} non-linear least-
174 squares optimization, using a non-negative least-squares (NNLS) fit²²⁻²⁴ to determine the metab-
175 olite amplitudes and baseline coefficients at each iteration of the non-linear optimization. Ampli-
176 tude ratio soft constraints are imposed on MM and lipid amplitudes, as well as selected pairs of

177 metabolite amplitudes, as defined in the LCMModel manual^{4,18}. The strength factor of the ampli-
 178 tude ratio soft constraint λ is set to 0.05 by default.

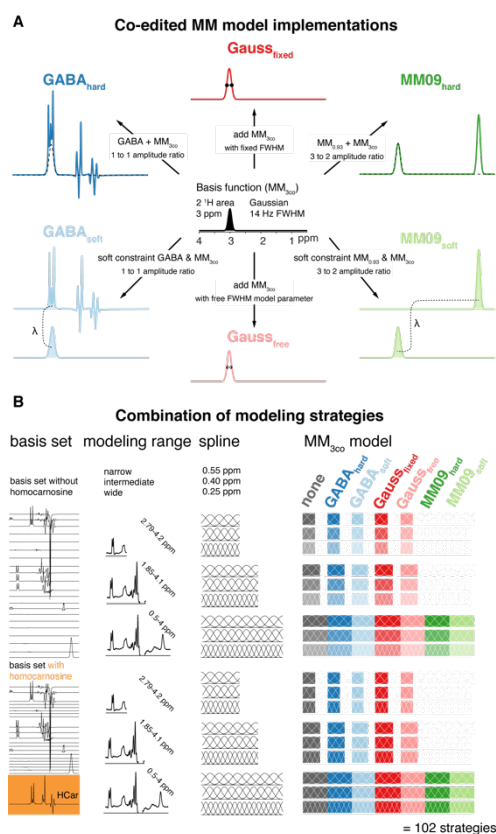


Figure 1 – Different linear combination modeling strategies for GABA-edited spectra. (A) Different co-edited MM_{3co} modeling approaches derived from a Gaussian function at 3.0 ppm (B) All combinations of basis set composition, modeling range, spline knot spacing, and MM_{3co} modeling leading to 102 different modeling strategies.

179 A range of modeling strategies for the GABA-edited difference spectrum was included in this
 180 study, covering various aspects of the modeling process (**Figure 1**). The different parametriza-
 181 tions and soft constraints to account for the co-edited MM_{3co} signal are shown in **Figure 1A**. All
 182 possible combinations for the modeling strategies: i) inclusion of homocarnosine in the basis set;
 183 ii) different parametrizations and soft constraints to account for the co-edited MM_{3co} signal; iii)
 184 different modeling ranges and iv) different baseline spline knot spacings (**Figure 1 B**). Each
 185 modeling aspect is described in detail below:
 186

187 Co-edited macromolecule models

188 Seven different strategies to model the GABA-edited difference spectrum were implemented
189 (**Figure 1 A**). The trivial approach – not accounting for the co-edited signal MM_{3co} at all – is la-
190 beled **none**. The other six modeling strategies all include a dedicated parametrized Gaussian
191 MM_{3co} basis function. This basis function is given different degrees of freedom in the different
192 strategies, e.g. hard- or soft-constrained relative to the amplitude of the GABA or the $MM_{0.94}$ ba-
193 sis functions, and with a fixed or free width. Here, strategies with fewer degrees of freedom re-
194 flect frequently the made assumptions that the GABA-to-MM ratio (and the MM background it-
195 self) are relatively stable across subjects, while strategies with more degrees of freedom or soft
196 constraints relax these assumptions:

- 197 • The **GABA_{hard}** model uses a single composite GABA+MM basis function by adding the
198 GABA and MM_{3co} (FWHM = 14 Hz) basis functions with a fixed 1:1 amplitude ratio. The
199 1:1 ratio reflects the widely used empirical assumption that 50% of the 3-ppm signal in a
200 conventional GABA-edited difference spectrum can be attributed to co-edited
201 macromolecules^{6,19}.
- 202 • The **GABA_{soft}** model uses separate GABA and MM_{3co} (FWHM = 14 Hz) basis functions, and
203 imposes a soft constraint on the ration of the amplitudes of both basis functions during the
204 optimization (1:1 ratio).
- 205 • The **Gauss_{fixed}** model uses separate GABA and MM_{3co} (fixed FWHM = 14 Hz) basis
206 functions. No further constraints are imposed. This means possible changes in the
207 contributions to the 3-ppm GABA peak are modeled.
- 208 • The **Gauss_{free}** model uses separate GABA and MM_{3co} basis functions. In contrast to the
209 Gauss_{fixed} model, the FWHM of the Gaussian MM_{3co} signal is represented by an additional
210 model parameter. This means that the MM_{3co} basis function itself is not static, but
211 dynamically modified during optimization.
- 212 • The **MM09_{hard}** model uses separate GABA and MM basis functions. The MM_{3co} basis
213 function is replaced by a composite $MM_{0.94} + MM_{3co}$ basis function (i.e., the fixed $MM_{0.94}$
214 (fixed FWHM = 11 Hz) and MM_{3co} (fixed FWHM = 14 Hz) basis functions are added in a
215 3:2 ratio).

- 216 • The **MM09_{soft}** model uses separate GABA, MM_{0.94} and MM_{3co} basis functions. In contrast to
217 the MM09_{hard} model, soft constraints enforce a ~3:2 amplitude ratio for the MM_{0.94} and
218 MM_{3co} amplitudes during optimization.

219 The models Gauss_{fixed}, MM09_{hard} and MM09_{soft} correspond to models previously investigated us-
220 ing the LCModel software²⁵ and the amplitude assumptions were derived empirically.

221

222 Varying the modeling range and baseline knot spacing

223 Two aspects of linear combination modeling are suggested to have a considerable influence on
224 metabolite estimates^{7,26}. First, the choice of the modeling range, i.e., the frequency interval that
225 defines the part of the frequency-domain spectrum that is considered to calculate the least-
226 squares difference between model and data. Second, the baseline knot spacing, i.e., the frequency
227 difference between two adjacent knots of the cubic spline basis that is used to approximate the
228 smooth baseline.

229

230 Three different modeling range scenarios were considered, reflecting common choices in the lit-
231 erature and widely used software tools: a) a wide modeling range typically used to analyze uned-
232 ited spectra, including all signals in the GABA-edited difference spectrum (0.5 to 4 ppm –
233 “wide”); b) an intermediate modeling range excluding signals below 1.9 ppm (e.g. co-edited li-
234 pids and macromolecules), but including strong co-edited signals from NAA, NAAG, Glu, Gln,
235 and GSH (1.85 and 4.1 ppm, “intermediate”), comparable to the range recommended in
236 LCModel; and c) a narrow modeling range only including the co-edited signals from GABA+
237 and Glx (2.79 – 4.2 ppm, “narrow”), the default modeling range in Gannet².

238

239 Three spline knot spacings were included in the analysis, with 0.4 ppm being the default Osprey
240 option, shown to create reproducible and comparable metabolite estimates for conventional MRS
241 ²⁷, as well as sparser (0.55 ppm) and denser (0.25 ppm) spline knot spacings.

242

243 Including homocarnosine in the basis set

244 To assess the effects of including homocarnosine in the linear combination model, we repeated
245 all analysis steps with two different basis sets: the default Osprey basis set *with* and *without* an
246 additional HCar basis function. Chemical shift and scalar coupling parameters describing the
247 HCar spin system were taken from literature⁶.

248
249 Combining the various MM_{3co} models (5 + 2 that were used for the wide modeling range only),
250 modeling ranges (3), baseline spline knot spacings (3), and basis sets (2), a total of 102 different
251 modeling strategies were investigated in this study. All models were implemented in Osprey¹²
252 and are available on GitHub¹³.

253

254 Quantification, visualization, and statistics

255 Quantification

256 For the basis set without homocarnosine, GABA refers to the model amplitude estimate for the
257 GABA basis function, which is of course only available for the modeling strategies with separate
258 basis functions for GABA and MM_{3co} (none, GABA_{soft}, Gauss_{fixed}, Gauss_{free}, MM09_{soft}). GABA+
259 refers to the sum of the amplitude estimates for GABA and MM_{3co} (GABA_{soft}, Gauss_{fixed}, Gauss-
260 _{free}, MM09_{hard}, MM09_{soft}) or the amplitude estimate for the composite basis function including
261 both MM and GABA (GABA_{hard}), and is therefore calculated for all strategies with an explicit
262 MM_{3co} model. The GABA amplitude for the `none` strategy is reported at GABA+.

263 For the basis set that included homocarnosine (HCar), the difference in GABA and MM_{3co} esti-
264 mates between the modeling strategies with and without HCar (Δ GABA and Δ MM_{3co}, respec-
265 tively) were investigated to evaluate whether the inclusion of HCar has a systematic effect on the
266 estimation of those signals with which it overlaps. edit-OFF spectrum over the wide modeling
267 range with a spline knot spacing of 0.4 ppm. Differences in GABA(+)/tCr between modeling
268 strategies are therefore only related to the modeling of the difference spectra, but not to the refer-
269 ence compound modeling. No further tissue or relaxation corrections were applied.

270 Further, the relative contributions of MM_{3co} to the GABA+ estimate and the relative contribu-
271 tions of HCar to the sum of GABA+ and HCar estimate were calculated.

272

273 Visualization

274 The modeling performance and systematic characteristics of each modeling strategy were visu-
275 ally assessed through the mean data, mean fit, mean residual, and mean models of GABA+,
276 GABA, MM_{3co}, HCar (if included) and the baseline, i.e., averaged across all datasets.

277
278 The metabolite estimate distributions were visualized as violin plots including boxplots with me-
279 dian, 25th/75th quartile ranges, and smoothed distributions to identify systematic differences be-
280 tween modeling strategies. In addition, the mean value of the models *without* a co-edited MM
281 model was added as a horizontal line. Bar plots were created to visualize quality metrics, includ-
282 ing the standard deviation if appropriate. All plots were generated with R²⁸ (Version 3.6.1) in
283 RStudio (Version 1.2.5019, RStudio Inc.) using SpecVis^{27,29}, an open-source package to visual-
284 ize linear combination modeling results with the ggplot2 package³⁰. All scripts and results are
285 publicly available³¹.

286

287 Statistics

288 Significant differences in the mean and the variance of the GABA, GABA+, and MM_{3co} esti-
289 mates were assessed between all modeling strategies. The statistical tests were set up as paired
290 without any further inference. Differences of variances were tested with Fligner-Killeen's test,
291 with a post-hoc pair-wise Bonferroni-corrected Fligner-Killeen's test. The means were compared
292 with an ANOVA or a Welch's ANOVA, depending on whether variances were different or not.
293 Post-hoc analysis was performed with a paired t-test with equal or non-equal variances, respec-
294 tively.

295

296 Model evaluation criteria

297 The performance of each modeling strategy was evaluated in different ways, including the im-
298 pact of the different modeling strategies on the GABA, GABA+ , and MM_{3co} estimates, as well
299 as several quality measures:

- 300 1) Visual inspection: Mean model, residual, and baseline were assessed for characteristic
301 features.
- 302 2) Range fit quality: the difference between the maximum and minimum of the residual was
303 determined, and then normalized by the noise level²⁶ (calculated as the standard

- 304 deviation of the noise between -2 and 0 ppm). This was done over the entire modeling
305 range of the difference spectrum and termed **residual_{range}**.
- 306 3) 3-ppm peak fit quality: Similar to the second criterion, the residual was calculated over
307 the range of 3.027 ± 0.15 ppm to assess the fit quality of the 3-ppm GABA peak and
308 termed **residual_{3ppm}**.
- 309 4) Consistency of metabolite estimates: Coefficients of variation for all metabolite estimates
310 (GABA/tCr, GABA+/tCr) were calculated for each modeling strategy.
- 311 5) Akaike Information Criterion (AIC): The Akaike information criterion ³², which takes the
312 number of model parameters into account, is defined as follows:

$$AIC_i = -2 \log(SSE_i) + 2K_i$$

313 Here, SSE_i is the sum of squared error/residual of modeling strategy i , and K_i is the num-
314 ber of free model parameters for that strategy. Soft constraint model parameters were in-
315 cluded with a value of 0.5. Lower AIC_i values indicate a more appropriate model. Subse-
316 quently, ΔAIC_i scores were calculated as the difference of AIC_i of modeling strategy i
317 and the model with the lowest AIC_{min} :

$$\Delta AIC_i = AIC_i - AIC_{min}$$

320

321 Results

322 All 62 datasets were successfully processed and modeled with all 102 modeling strategies. No
323 data were excluded from further analysis.

324 Summary and visual inspection of the modeling results

325

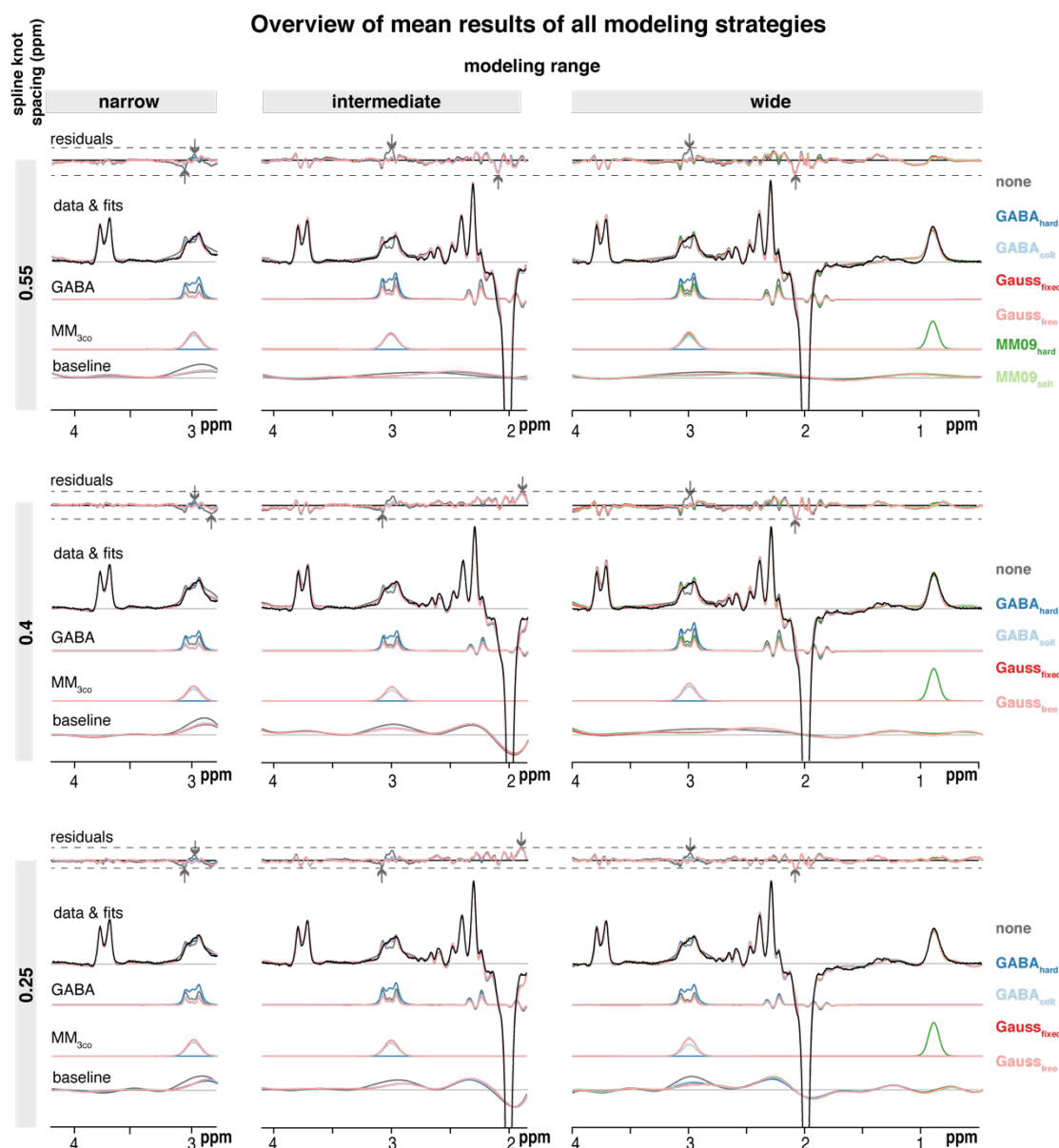
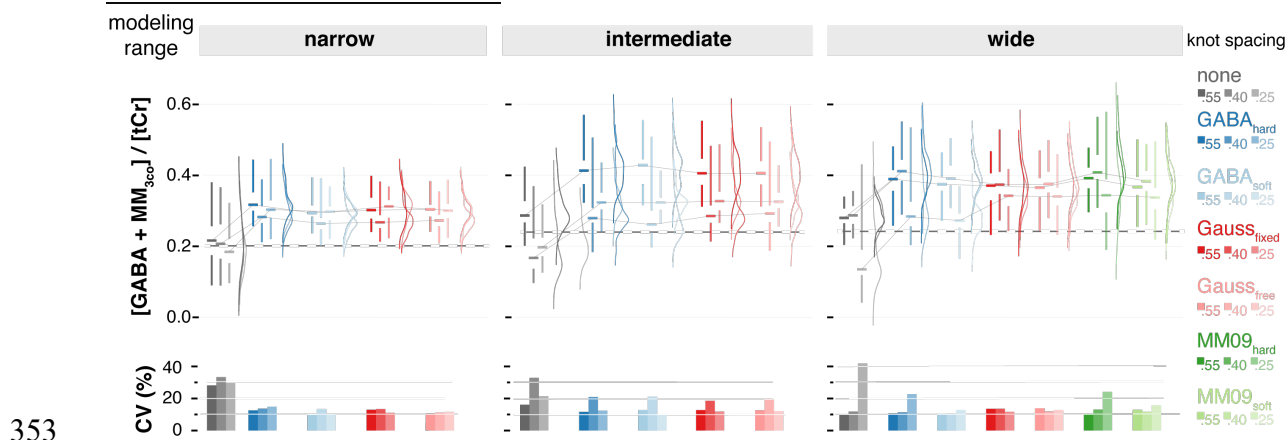


Figure 2 – Mean modeling results for all modeling strategies without homocarnosine. A substantial structured residual is apparent at 3 ppm if no MM modeling strategy is included. All three modeling ranges (columns), three spline knot spacings (rows), and MM_{3co} model (color-coded) are presented with mean residuals and fits, as well as the GABA⁺, GABA, MM_{3co}, and spline baseline models. The mean data is included in black. The dashed lines indicate the range

of the residual across one row and the arrows indicate the maximum of a specific modeling range and spline knot spacing (color-coded).

327
328 **Figure 2** shows the mean modeling results for all modeling strategies without homocarnosine.
329 Not including MM_{3co} leads to a substantial structured residual around 3 ppm for all knot spacings
330 and modeling ranges. In contrast, all modeling strategies with MM_{3co} appear to reflect the line-
331 shape of the 3-ppm signal more accurately, with very similar results for the complete fit (metabo-
332 lites, MMs, and baseline) and the individual components. Modeling strategies with the interme-
333 diate and wide modeling range further show strong residuals around 2 ppm, suggesting slightly
334 inaccurate lineshape modeling of the methyl singlets from NAA and NAAG, or inaccurate mod-
335 eling of co-edited MM signals in this region. Structured residuals appear also in the region of the
336 3.75 ppm Glx signals, although they are much less pronounced in strategies with the narrow
337 modeling range, suggesting that including the 2.25 ppm multiplets (and underlying baseline fluc-
338 tuation) has a considerable impact on phase estimation.
339 In general, the residuals are consistent between different MM_{3co} models for any given knot spac-
340 ing and modeling range. Notably, residuals tend to be smaller for denser knot spacing and nar-
341 rower modeling range.
342 Mean GABA models agree well between all strategies with a separate MM_{3co} model. The
343 GABA_{hard} strategy appears to produce a larger signal as its GABA basis function includes the
344 MM_{3co} signal, but does not model it separately, while the strategies that do so produce compara-
345 ble mean MM_{3co} models.
346 The mean baseline is consistently flatter around 3 ppm for modeling strategies with an explicit
347 MM_{3co} model, while absorbing substantially more signal for the ‘none’ approach without an MM
348 model. This behavior is particularly obvious for the dense knot spacing (0.25 ppm) over the wide
349 modeling range. Baseline curvature generally increases for denser knot spacings around 2.2 ppm
350 for the intermediate and wide range.
351

352 Metabolite level distribution



353 *Figure 3 – Distribution and coefficients of variation (CVs) of GABA+ estimates for all modeling strategies. Including a MM_{3co} model significantly increases the mean estimates for all modeling strategies, while giving similar or reduced CVs. All three modeling ranges (column) and three spline knot spacings (within each column), and co-edited MM models (color-coded) are presented. Distributions are shown as half-violins (smoothed distribution), box plots with median, interquartile range, and 25th/75th quartile. CVs are summarized as bar plots.*

354 **Figure 3** shows distributions and coefficients of variation (CVs) of the GABA+ estimates for all
 355 modeling strategies. GABA+ estimates are significantly higher than GABA-only estimates of the
 356 ‘none’ modeling strategy for all modeling ranges and knot spacings, supporting the notion from
 357 **Figure 2** that not including an MM model leaves a considerable fraction of the edited 3-ppm sig-
 358 nal unmodeled, resulting in substantial residuals or increased baseline amplitudes flexion. Nota-
 359 bly, CVs for the strategies including MM models are comparable or reduced.

360 All modeling strategies with MM_{3co} model return comparable mean estimates and CVs within
 361 the same knot spacing. In addition, sparser knot spacing leads to lower CVs. The intermediate
 362 modeling range does not appear to perform more consistently than both other modeling ranges.
 363

364

365 Model evaluation

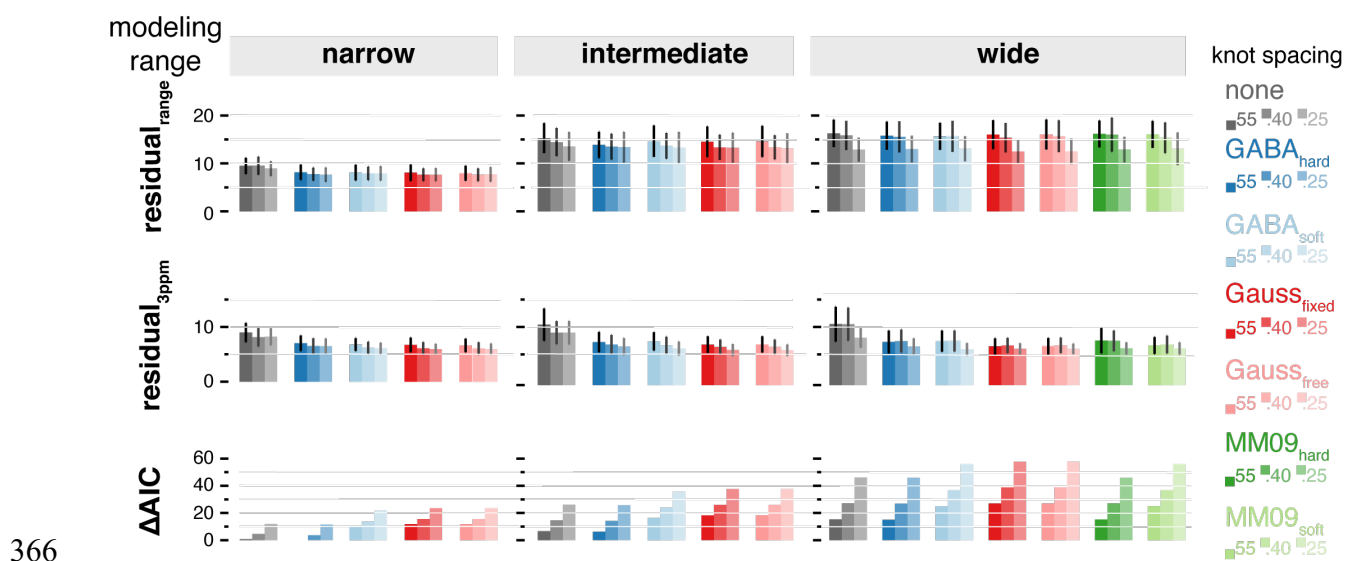


Figure 4 – Evaluation of all modeling strategies. Including an MM_{3co} model reduces the 3-ppm residual by ~30% without significant impact on the ΔAIC . All three modeling ranges (column) and three spline knot spacings (within each column), and co-edited MM models (color-coded) are presented. Bar plots represent mean values; SD is indicated by whiskers where appropriate.

367 **Figure 4** summarizes the metrics used for model evaluation. The residual over the modeled fre-
 368 quency range ($residual_{range}$) is lowest for the narrow modeling range. For the intermediate and
 369 wide modeling ranges, $residual_{range}$ is substantially higher, largely driven by the 2-ppm region
 370 (see also **Figure 2**). Consequentially, $residual_{range}$ is comparable between MM modeling strate-
 371 gies for a given knot spacing.

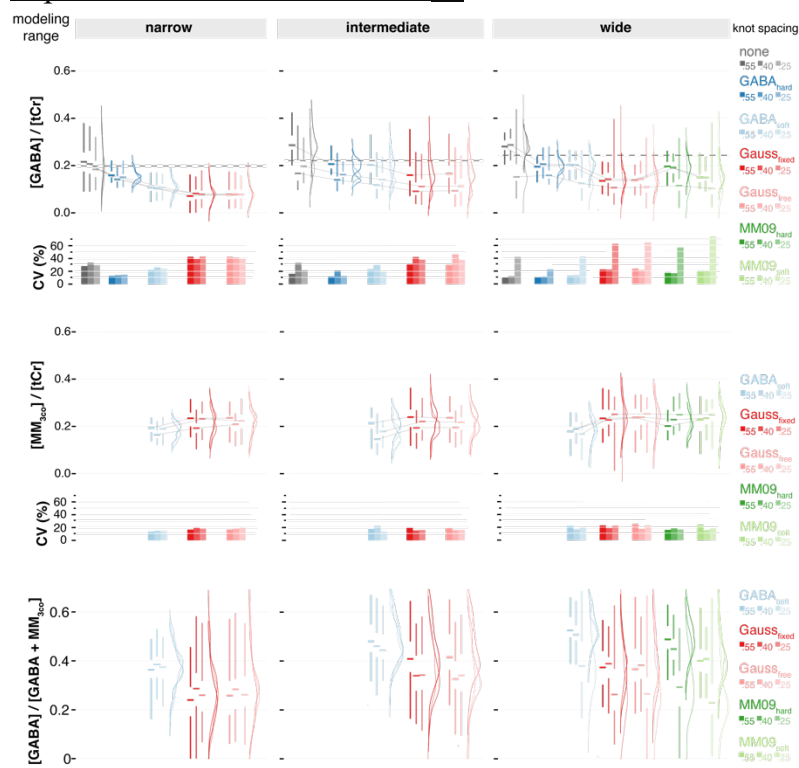
372 The residual around the GABA⁺ peak ($residual_{3ppm}$) is consistently reduced by up to 30% if a
 373 MM_{3co} model is included, in line with the reduction of structured residual in **Figure 2**. This ef-
 374 fect is less pronounced for the dense knot spacing (0.25 ppm), indicating that a flexible baseline
 375 is to some degree capable of accounting for otherwise unmodeled MM signal. Together, these
 376 findings again support the notion that omitting an explicit MM_{3co} model does not capture the
 377 whole edited 3-ppm signal, which remains unmodeled (in the residual) or gets partially absorbed
 378 by the baseline or interpreted incorrectly as GABA signal.

379 The strategy with the lowest AIC is the GABA_{hard} model with the narrow modeling range and
 380 sparse knot spacing, reflecting the low number of model parameters: there is no separate basis

381 function for MM, and the lowest possible number of splines. The Δ AIC (the difference between
382 the lowest AIC and the individual model's AIC) consequently increases for larger modeling
383 ranges, as more splines are included. Similarly, Δ AIC increases for denser knot spacings, and in
384 fact, this increase is much stronger compared to the resulting reduction in both residual
385 measures, suggesting that the increased flexibility and reduction of the residual does not justify
386 the greater number of model parameters.

387 For any given knot spacing and modeling range, Δ AIC are comparable between MM_{3co} models,
388 with moderate increases when more parameters are estimated. Together with its low CV for
389 GABA+, the Δ AIC for the MM09_{hard} model over the wide modeling range with sparse knot spac-
390 ing (Δ AIC = 15.4) indicates a good performance of this particular model without introducing
391 overfitting.

392 Separation of GABA and MM_{3co}



393

Figure 5 - Distribution of GABA and MM_{3co} estimates and the relative contribution of GABA to GABA+ for all modeling strategies. All three modeling ranges (column) and three spline knot spacings (within each column), and MM_{3co} models (color-coded) are presented. Distributions are shown as half-violins (smoothed distribution), box plots with median, interquartile range, and 25th/75th quartile. CVs are summarized as bar plots.

Figure 5 shows the distributions and CVs of the separate GABA and MM_{3co} estimates of all modeling strategies. Including a separate MM_{3co} basis function significantly decreases GABA estimates, suggesting that not doing so may lead to GABA overestimation, as MM signal is mistakenly modeled as GABA. As was seen for the composite GABA+ estimates in **Figure 3**, sparser knot spacing appears to stabilize modeling, leading to lower CVs of GABA. This becomes especially obvious for the wide modeling range, where GABA CVs exceed 50% for dense knot spacing.

MM_{3co} estimates are stable across the different knot spacings, suggesting that the different parametrizations accurately account for most of the co-edited MM signal at 3 ppm.

The GABA_{soft} model, in combination with a wide modeling range and 0.55 ppm knot spacing, exhibits the lowest CV for GABA (12.9%). However, the MM09_{hard} model in combination with

the same knot spacing and modeling range has comparable GABA CVs (17.3%). The corresponding MM_{3co} CVs were 22.6% (GABA_{soft}) and 16.2% (MM09_{hard}), respectively. One might argue that it is beneficial to opt for the MM09_{hard} model, since the MM_{0.94} peak provides an ‘external’, non-overlapped reference anchor for the expected MM₃₀ peak – the MM landscape is thought to be relatively stable across subjects, at least in the absence of pathology⁸. Furthermore, the MM09_{hard} model does not impose any amplitude assumptions or constraints on GABA. **Supplementary Material 2** reports the mean and SDs of the GABA+, GABA, and MM_{3co} estimates. Significant differences between the mean or the SD compared to the corresponding model omitting co-edited MMs are indicated bold.

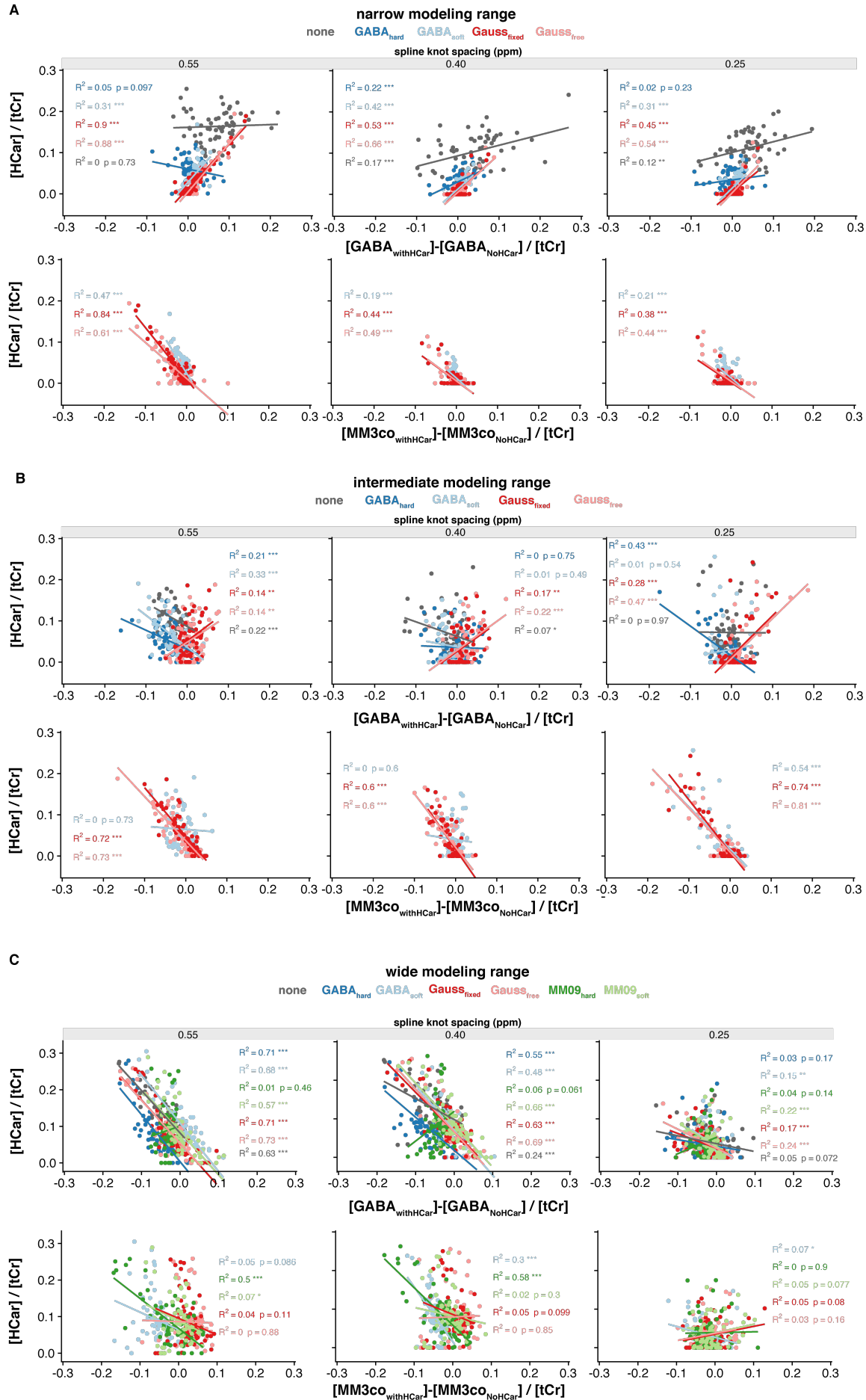


Figure 6 – Impact of including homocarnosine in the basis set. The directionality of the correlation indicates that HCar absorbs GABA signal specifically for the intermediate and wide modeling range and absorbs MM_{3co} signal for all modeling ranges. Correlation analysis between the differences between GABA/ MM_{3co} estimates with and without HCar in the basis set and the HCar estimates. All three modeling ranges (column) and three spline knot spacings (within each column) were investigated. Pearson's correlation was calculated for each MM_{3co} model (color-coded).

395 Finally, **Figure 6** shows the impact of including HCar into the basis set with the difference in
396 GABA and MM_{3co} estimates between the modeling strategies with and without HCar (Δ GABA
397 and Δ MM_{3co}, respectively). Interestingly, clear differences in the systematic effects of HCar are
398 evident between the modeling ranges:
399 For the narrow modeling range (**Figure 6 A**), HCar estimates correlate positively with Δ GABA,
400 but the correlation is *only* substantial for strategies with a *separate* MM basis function. For
401 precisely these strategies, HCar estimates correlate negatively with Δ MM_{3co}. These observations
402 suggest that HCar is likely to account for MM_{3co} in the narrow modeling range. In contrast, HCar
403 and Δ GABA correlate negatively for most strategies in the intermediate and wide modeling
404 ranges (**Figure 6 B and C**). The negative correlations between HCar and Δ MM_{3co} and are
405 notably weaker for these modeling ranges, indicating that HCar is more likely to account for
406 GABA signal instead of MM.
407 This behavior can possibly be explained by the HCar signal shape for each modeling range
408 (**Supplementary Material 3**). For the narrow modeling range, the HCar basis function offers the
409 model an additional degree of freedom to account for deviations of the actual edited 3-ppm
410 signal from pure GABA and the symmetric Gaussian MM_{3co} component, as no resonances
411 below 2.78 ppm are considered. As a result, HCar shows a high correlation with the difference in
412 MM_{3co}. For the intermediate and wide range, the HCar basis function resembles the GABA basis
413 function since other resonances are included, effectively coupling GABA and HCar estimates to
414 each other. Perhaps unsurprisingly, HCar estimates are significantly higher for 'none' modeling
415 strategy, and are substantially lower for more flexible baselines, supporting the notion that HCar
416 rather serves as a substitute for an explicit MM signal, in particular if the baseline cannot absorb
417 the latter (**Supplementary Material 3**). Within a given knot spacing and modeling range, HCar
418 estimates are comparable between different MM_{3co} models, a behavior observed for GABA
419 estimates as well.

420 The GABA+ + homocarnosine estimates show a slight increase compared to the GABA+
421 estimates without HCar (**Supplementary Material 4**). For the ‘none’ model, stronger changes
422 occur as HCar accounts for MM signal (see also Figure 6). There was no improvement in the
423 CVs observed when including HCar in the model. The relative contribution of HCar to GABA+
424 ranged between 2.2% and 19.1% for modeling strategies with an MM_{3co} basis function and
425 between 18% and 36% for the ‘none’ model.
426

427 **Discussion**

428 The application of linear combination modeling to edited difference spectra is neither straightfor-
429 ward nor intuitive. The conceptual advantage of spectral editing arises from isolating a resolved
430 target resonance, i.e. reducing the overlap of the target metabolite with other signals, as well as
431 the number of signals in the spectrum in general¹. LCM, on the other hand, benefits from maxim-
432 izing the use of prior knowledge to solve the spectral modeling problem, i.e. using all available
433 information for meaningful constraint, including from overlapping signals. The specific case of
434 GABA-edited MRS at 3T poses unique and unresolved challenges. Firstly, a compromise must
435 be drawn between maximizing the prior knowledge by increasing the modeling range and reduc-
436 ing the impact of co-edited and unwanted signals. Secondly, an appropriate parametrization of
437 poorly characterized co-edited signals must be found, and possible interactions with the target
438 metabolite GABA must be evaluated. Thirdly, effects of baseline modeling must be studied,
439 again a consequence of the macromolecular background signal in the GABA-edited difference
440 spectrum not being determined to this date. In this study, a total of 102 linear combination mod-
441 eling strategies were compared for GABA-edited difference spectra, each with different model-
442 ing ranges, parametrizations of co-edited signals, and baseline model flexibility. The key find-
443 ings are:

- 444 • Including a dedicated basis function for co-edited MM improves fit residuals,
445 reduces CVs of GABA and GABA⁺ estimates, and avoids overestimation of
446 GABA.
- 447 • Reducing the modeling range does not substantially stabilize or destabilize
448 modeling, while removing potentially valuable information (MM_{0.93} and 2-ppm
449 NAA peak) from the optimization.
- 450 • Sparser baseline spline knot spacing leads, on average, to the lowest CV across all
451 modeling ranges.
- 452 • GABA and MM_{3co} show a stable separability by linear combination modeling,
453 and stable MM_{3co} estimates indicate appropriate parametrization within each M_{3co}
454 parametrization.

455 There is surprisingly little systematic investigation into linear combination modeling of GABA-
456 edited difference spectra. To the best of our knowledge, there is only one conference abstract

457 studying MM parametrization in GABA-edited MRS with the LCModel software²⁵. The results
458 from this preliminary investigation indicate that including a specific MM basis function signifi-
459 cantly reduces GABA estimates, which our findings confirm.

460
461 Although the substantial contribution of broad MM signals to the 3-ppm peak in the GABA-ed-
462 ited spectrum is widely known^{1,33}, it is rarely explicitly addressed in linear combination model-
463 ing. Instead, it is assumed that either an incomplete model (without explicit MM term) will still
464 provide an accurate GABA estimate, or that baseline modeling will account for the MM signal.
465 The current results provide evidence that including an appropriately parametrized MM model is
466 a preferable and easily implemented strategy, reducing the residual over the 3-ppm signal range
467 by up to 30%, with similar or lower CVs for GABA+. In contrast, not including an MM model
468 likely causes systematic overestimation of GABA, as the least-squares optimization attempts to
469 minimize the model-data difference with an inadequate set of basis functions (only GABA), par-
470 ticularly when a rigid baseline is chosen. Including MM_{3co} is a justified and reasonable measure
471 without overfitting (reflected by AIC), and stable mean estimates and CVs of MM_{3co} suggest an
472 adequately parametrized model.

473
474 The different MM models in this study were based on certain assumptions, including the relative
475 contribution of MM_{3co} to the 3-ppm GABA peak to be around 50%^{1,6,8,19}. Levels of MM_{0,93} have
476 been found to be stable across the whole brain³⁴ and are thought to be stable across healthy sub-
477 jects. Under these assumptions, the MM09_{hard} model with a rigid amplitude coupling between
478 MM_{3co} and the non-overlapped MM_{0,93} peak is a suitable strategy, supported by favorable CVs
479 and Δ AIC. Further studies need to be performed to investigate the distribution and correlation
480 between MM_{0,93} and MM_{3co} in the brain.

481
482 Unedited MRSI data measured at 7T indicates significant differences between white and gray
483 matter for several macromolecules in the healthy brain³⁴. Changes in the MM concentrations dur-
484 ing disease may also affect the relative contribution to the 3-ppm peak, and therefore render
485 models with prior amplitude assumptions inaccurate. If there is reason to expect strong fluctua-
486 tions of MM_{3co}, a modeling strategy with fewer assumptions about amplitude ratios between the
487 metabolite of interest GABA or the MM_{0,93} signal and the MM_{3co} signal is preferable to the

488 MM09_{hard} strategy. Here, the Gauss_{free} and Gauss_{fixed} strategies could be used to account for
489 changes in the MM_{3co} contribution more freely, as their mean estimates of GABA and GABA+
490 were in good agreement with the more constrained approaches, although they led to increased
491 CVs and Δ AICs. In addition, the less-constrained models are available for model-based investi-
492 gations of changes in MM_{3co} due to age³⁵ or disease, and may offer a parametrization of fre-
493 quency-drift-related effects on the co-edited MM signal^{1,8,36}. Another potential way to model the
494 co-edited MM signal is to include lysine in the simulated basis set, as it has been identified as the
495 potential source of the signal⁶, although this approach would require appropriate broadening and
496 incorporation of chemical shift and coupling values from protein databases³⁷.

497
498 Overall, results did not differ drastically between modeling ranges, although it is noteworthy that
499 the effects of baseline flexibility were less pronounced for the narrow modeling range, likely be-
500 cause the complex interaction of the overlapping 2.25 ppm GABA and Glx signals with the un-
501 derlying baselines is omitted. Furthermore, there was no evidence that the intermediate modeling
502 range, which is proposed in the LCMoel manual¹⁸ to avoid frequently occurring co-edited lipid
503 signals, improved quantification substantially compared to both other modeling ranges, although
504 it should be mentioned that this particular dataset did not suffer from severe lipid contamination.
505 Taken together, the choice of modeling range does not impact quantitative results as substantially
506 as the inclusion of an MM model.

507
508 Baseline models are included in most LCM algorithms to account for signals not otherwise mod-
509 eled, e.g. residual water tails or unparametrized macromolecules and lipids. Compared to con-
510 ventional short-TE spectra, water and non-co-edited MMs are removed upon subtraction in the
511 GABA-edited spectrum, which is therefore frequently modeled with a stiffer baseline^{4,18}. Our re-
512 sults show that sparser knot spacing (0.55 ppm) leads to lower CVs in metabolite estimates. A
513 more flexible baseline (0.25 ppm) improves local and global residuals, but not enough to justify
514 the additional model parameters (as per the AICs). More importantly, an overly flexible baseline
515 may absorb edited signal, although it appeared that it did not do so excessively even for the 0.25-
516 ppm strategies. The exception was the ‘none’ model, where the baseline was the only available
517 part of the model to take up signal, underlining the inadequacy of the default LCMoel approach.
518 Taken together, a relatively rigid baseline with a parametrized MM basis function is preferable

519 for LCM of GABA-edited spectra. A caveat to this recommendation is the observation of struc-
520 tural baseline fluctuations underneath the 2.25 ppm signals from GABA, Glx, GSH, NAA and
521 NAAG, particularly for the 0.25 ppm knot spacing. These were observed previously²⁵, and are
522 likely signals from un-parametrized MMs directly and indirectly affected by the editing pulse.
523 Rigid baselines may force a wrong metabolite model in that region and interfere with accurate
524 estimation of GABA and Glx. In fact, the structural Glx residual at 3.75 ppm suggests a system-
525 atic misestimation of the Glx phase, likely driven by the 2.25 ppm signals. While beyond the
526 scope of this investigation, it is conceivable that more informed parametrization (or, ideally, di-
527 rect measurement) of this unexplored MM background may benefit the modeling of the entire
528 difference spectrum. Alternatively, hitherto unexplored approaches with variable baseline knot
529 spacing may be worth investigating.

530
531 The HCar molecule has a GABA moiety with similar chemical shifts and is therefore co-edited.
532 Evidence regarding in-vivo HCar levels in the human brain is inconclusive – early work deter-
533 mined HCar levels to be 0.5 mM⁵ (compared to ~1 mM for GABA), while a recent hybrid up-
534 field/downfield inversion-recovery method determined the HCar/GABA ratio as 17%³⁸. There-
535 fore, we tested the impact of adding HCar to the basis set without additional constraints. Includ-
536 ing HCar systematically affected GABA and MM_{3co} estimates, in a way that strongly depended
537 on the choice of modeling range. HCar estimates themselves ranged from 2.2% to 19.1% of the
538 GABA+ signal, depending strongly on the degree of baseline flexibility. The results suggest that
539 the overlap between the three model terms (HCar, GABA, MM_{3co}) is too substantial for reliable
540 three-way separation, particularly in the presence of a highly flexible baseline. A minor increase
541 in “GABA+ plus HCar” estimates compared to GABA+ estimates was observed and the inclu-
542 sion of HCar did not substantially improve the CVs. Additionally, the disagreement between the
543 model and the data at 2.9 ppm indicates that a simple unconstrained addition of HCar to the mod-
544 eling is not justified.

545
546 A limitation of this study is the high spectral quality (SNR, linewidth, no apparent subtraction
547 artefacts, or lipid contaminations) of the dataset analyzed. We did not investigate model para-
548 metrizations of movement or drift, which may introduce systematic changes to the co-edited MM
549 signal. While our results suggest that using the wide modeling range with a rigid baseline is

550 beneficial, strong co-edited lipid signals are likely to not be modeled appropriately, and the inter-
551 mediate modeling range may be more suitable. Further studies of the possible impact of changes
552 in spectral quality need to be performed to validate the modeling strategies under suboptimal
553 conditions.

554 **Conclusion**

555 This study proposed and compared different modeling strategies for LCM of GABA+-edited dif-
556 ference spectra from a multi-site MEGA-PRESS dataset. Introducing a parametrized model for
557 co-edited macromolecules reduces fit residuals, while maintaining low coefficients of variation
558 of GABA+ estimates. Under certain conditions, it was found that GABA and co-edited MM are
559 separated in a stable way. A rigid baseline was found to be beneficial, while using a narrower
560 modeling range did not significantly improve the modeling. The overall modeling results suggest
561 that GABA-edited data are reliably modeled with an adequately parametrized MM_{3co} model,
562 constrained by the non-overlapped 0.93-ppm MM resonance, in combination with a full model-
563 ing range and sparse knot spacing. Incorporating homocarnosine into the modeling did not sig-
564 nificantly improve the GABA+ estimates and did not allow for a stable separation of GABA and
565 HCar.

566 **References**

- 567 1. Choi I-Y, Andronesi OC, Barker P, et al. Spectral editing in ¹H magnetic resonance spectroscopy: Experts' consensus recommendations. *NMR Biomed.* 2021;n/a(n/a):e4411.
568 doi:<https://doi.org/10.1002/nbm.4411>
569
- 570 2. Edden RAE, Puts NAJ, Harris AD, Barker PB, Evans CJ. Gannet: A batch-processing tool
571 for the quantitative analysis of gamma-aminobutyric acid-edited MR spectroscopy spectra.
572 *J Magn Reson Imaging.* 2014;40(6):1445-1452. doi:10.1002/jmri.24478
- 573 3. Wilson M, Reynolds G, Kauppinen RA, Arvanitis TN, Peet AC. A constrained least-
574 squares approach to the automated quantitation of in vivo ¹H magnetic resonance spectroscopy
575 data. *Magn Reson Med.* 2011;65(1):1-12.
- 576 4. Provencher SW. Automatic quantitation of localized in vivo ¹H spectra with LCModel.
577 *NMR Biomed.* 2001;14(4):260-264. doi:10.1002/nbm.698
- 578 5. Petroff OAC, Hyder F, Rothman DL, Mattson RH. Topiramate Rapidly Raises Brain
579 GABA in Epilepsy Patients. *Epilepsia.* 2001;42(4):543-548.
580 doi:<https://doi.org/10.1046/j.1528-1157.2001.18800.x>
- 581 6. Deelchand DK, Marjańska M, Henry P-G, Terpstra M. MEGA-PRESS of GABA+: Influences
582 of acquisition parameters. *NMR Biomed.* 2019;n/a(n/a):e4199.
583 doi:<https://doi.org/10.1002/nbm.4199>
- 584 7. Marjańska M, Terpstra M. Influence of fitting approaches in LCModel on MRS quantification
585 focusing on age-specific macromolecules and the spline baseline. *NMR Biomed.* November
586 2019. doi:10.1002/nbm.4197
- 587 8. Shungu DC, Mao X, Gonzales R, et al. Brain γ -aminobutyric acid (GABA) detection in
588 vivo with the J-editing (¹H) MRS technique: a comprehensive methodological evaluation
589 of sensitivity enhancement, macromolecule contamination and test-retest reliability. *NMR
590 Biomed.* 2016;29(7):932-942. doi:10.1002/nbm.3539
- 591 9. Bhagwagar Z, Wylezinska M, Jezzard P, et al. Reduction in Occipital Cortex γ -Aminobutyric
592 Acid Concentrations in Medication-Free Recovered Unipolar Depressed and Bipolar
593 Subjects. *Biol Psychiatry.* 2007;61(6):806-812. doi:10.1016/j.biopsych.2006.08.048
- 594 10. Mikkelsen M, Barker PB, Bhattacharyya PK, et al. Big GABA: Edited MR spectroscopy at
595 24 research sites. *NeuroImage.* 2017;159:32-45. doi:10.1016/j.neuroimage.2017.07.021
- 596 11. Edden RAE, Oeltzschner G, Harris AD, et al. Prospective frequency correction for macro-
597 molecule-suppressed GABA editing at 3T. *J Magn Reson Imaging JMRI.* 2016;44(6):1474-
598 1482. doi:10.1002/jmri.25304
- 599 12. Oeltzschner G, Zöllner HJ, Hui SCN, et al. Osprey: Open-source processing, reconstruction
600 & estimation of magnetic resonance spectroscopy data. *J Neurosci Methods.*
601 2020;343:108827. doi:10.1016/j.jneumeth.2020.108827

- 602 13. Osprey GitHub repository. Osprey GitHub repository. <https://github.com/schorschinho/osprey>. Published 2020. Accessed May 27, 2020.
603
- 604 14. Klose U. In vivo proton spectroscopy in presence of eddy currents. *Magn Reson Med*.
605 1990;14(1):26-30. doi:10.1002/mrm.1910140104
- 606 15. Mikkelsen M, Tapper S, Near J, Mostofsky SH, Puts NAJ, Edden RAE. Correcting fre-
607 quency and phase offsets in MRS data using robust spectral registration. *NMR Biomed*. July
608 2020:e4368. doi:10.1002/nbm.4368
- 609 16. Barkhuijsen H, de Beer R, van Ormondt D. Improved algorithm for noniterative time-do-
610 main model fitting to exponentially damped magnetic resonance signals. *J Magn Reson*
611 1969. 1987;73(3):553-557. doi:10.1016/0022-2364(87)90023-0
- 612 17. Simpson R, Devenyi GA, Jezzard P, Hennessy TJ, Near J. Advanced processing and simu-
613 lation of MRS data using the FID appliance (FID-A)—An open source, MATLAB-based
614 toolkit. *Magn Reson Med*. 2017;77(1):23-33. doi:10.1002/mrm.26091
- 615 18. Provencher S. LCMModel & LCMgui User's Manual. LCMModel & LCMgui User's Manual.
616 <http://s-provencher.com/pub/LCMModel/manual/manual.pdf>. Published 2020. Accessed April
617 28, 2020.
- 618 19. Henry PG, Dautry C, Hantraye P, Bloch G. Brain gaba editing without macromolecule con-
619 tamination. *Magn Reson Med*. 2001;45(3):517-520. doi:10.1002/1522-
620 2594(200103)45:3<517::AID-MRM1068>3.0.CO;2-6
- 621 20. Levenberg K. A method for the solution of certain non-linear problems in least squares. *Q*
622 *Appl Math*. 1944;2(2):164-168. doi:10.1090/qam/10666
- 623 21. Marquardt DW. An Algorithm for Least-Squares Estimation of Nonlinear Parameters. *J Soc*
624 *Ind Appl Math*. 1963;11(2):431-441. doi:10.1137/0111030
- 625 22. Becker S. LBFGB (L-BFGS-B) mex wrapper - File Exchange - MATLAB Central.
626 LBFGB (L-BFGS-B) mex wrapper - File Exchange - MATLAB Central.
627 [https://www.mathworks.com/matlabcentral/fileexchange/35104-lbfgsb-l-bfgs-b-mex-wrap-](https://www.mathworks.com/matlabcentral/fileexchange/35104-lbfgsb-l-bfgs-b-mex-wrapper)
628 [per](https://www.mathworks.com/matlabcentral/fileexchange/35104-lbfgsb-l-bfgs-b-mex-wrapper). Published February 23, 2015. Accessed March 3, 2021.
- 629 23. Byrd RH, Lu P, Nocedal J, Zhu C. A Limited Memory Algorithm for Bound Constrained
630 Optimization. *SIAM J Sci Comput*. 1995;16(5):1190-1208. doi:10.1137/0916069
- 631 24. Zhu C, Byrd RH, Lu P, Nocedal J. Algorithm 778: L-BFGS-B: Fortran subroutines for
632 large-scale bound-constrained optimization. *ACM Trans Math Softw*. 1997;23(4):550-560.
633 doi:10.1145/279232.279236
- 634 25. Murdoch JB, Dydak U. Modeling MEGA-PRESS macromolecules for a better grasp of
635 GABA. In: *19th Annual Meeting of the International Society for Magnetic Resonance in*
636 *Medicine (ISMRM)*. ; 2011. [https://scholar.google.com/scholar_lookup?title=Model-](https://scholar.google.com/scholar_lookup?title=Modeling%20MEGA-)
637 [ing%20MEGA-](https://scholar.google.com/scholar_lookup?title=Modeling%20MEGA-)

- 638 PRESS%20macromolecules%20for%20a%20better%20grasp%20of%20GABA&publica-
639 tion_year=2011&author=J.B.%20Murdoch&author=U.%20Dydak. Accessed July 1, 2020.
- 640 26. Wilson M, Andronesi O, Barker PB, et al. *Methodological Consensus on Clinical Proton*
641 *MRS of the Brain: Review and Recommendations*. Vol 82. John Wiley and Sons Inc.; 2019.
642 doi:10.1002/mrm.27742
- 643 27. Zöllner HJ, Považan M, Hui SCN, Tapper S, Edden RAE, Oeltzschner G. Comparison of
644 different linear-combination modeling algorithms for short-TE proton spectra. *NMR Bio-*
645 *med*. 2021;n/a(n/a):e4482. doi:<https://doi.org/10.1002/nbm.4482>
- 646 28. R Core Team. *R: A Language and Environment for Statistical Computing*. Vienna, Austria:
647 R Foundation for Statistical Computing; 2017. <https://www.R-project.org/>.
- 648 29. SpecVis GitHub repository. SpecVis GitHub repository.
649 <https://github.com/hezoe100/SpecVis>. Published 2020. Accessed May 27, 2020.
- 650 30. Wickham H. *Ggplot2: Elegant Graphics for Data Analysis*. Springer-Verlag New York;
651 2009. <http://ggplot2.org>.
- 652 31. Zöllner HJ. Comparison of linear-combination modeling strategies for GABA-edited MRS
653 at 3T. <https://osf.io/aqm8f/>. Published April 30, 2021. Accessed April 30, 2021.
- 654 32. Akaike H. A new look at the statistical model identification. *IEEE Trans Autom Control*.
655 1974;19(6):716-723. doi:10.1109/TAC.1974.1100705
- 656 33. Cudalbu C, Behar KL, Bhattacharyya PK, et al. Contribution of macromolecules to brain
657 1H MR spectra: Experts' consensus recommendations. *NMR Biomed Revis*. 2020.
- 658 34. Považan M, Strasser B, Hangel G, et al. Simultaneous mapping of metabolites and individ-
659 ual macromolecular components via ultra-short acquisition delay 1H MRSI in the brain at
660 7T. *Magn Reson Med*. 2018;79(3):1231-1240. doi:10.1002/mrm.26778
- 661 35. Marjańska M, Deelchand DK, Hodges JS, et al. Altered macromolecular pattern and con-
662 tent in the aging human brain. *NMR Biomed*. 2018;31(2):e3865. doi:10.1002/nbm.3865
- 663 36. Veen JW van der, Marengo S, Berman KF, Shen J. Retrospective correction of frequency
664 drift in spectral editing: The GABA editing example. *NMR Biomed*. 2017;30(8):e3725.
665 doi:<https://doi.org/10.1002/nbm.3725>
- 666 37. Borbath T, Manohar SM, Henning A. Towards a Fitting Model of Macromolecular Spectra:
667 Amino Acids. In: *27th Annual Meeting of the International Society for Magnetic Resonance*
668 *in Medicine (ISMRM)*. Montreal, Canada; 2019.
- 669 38. Landheer K, Prinsen H, Petroff OA, Rothman DL, Juchem C. Elevated homocarnosine and
670 GABA in subject on isoniazid as assessed through 1H MRS at 7T. *Anal Biochem*.
671 2020;599:113738. doi:10.1016/j.ab.2020.113738

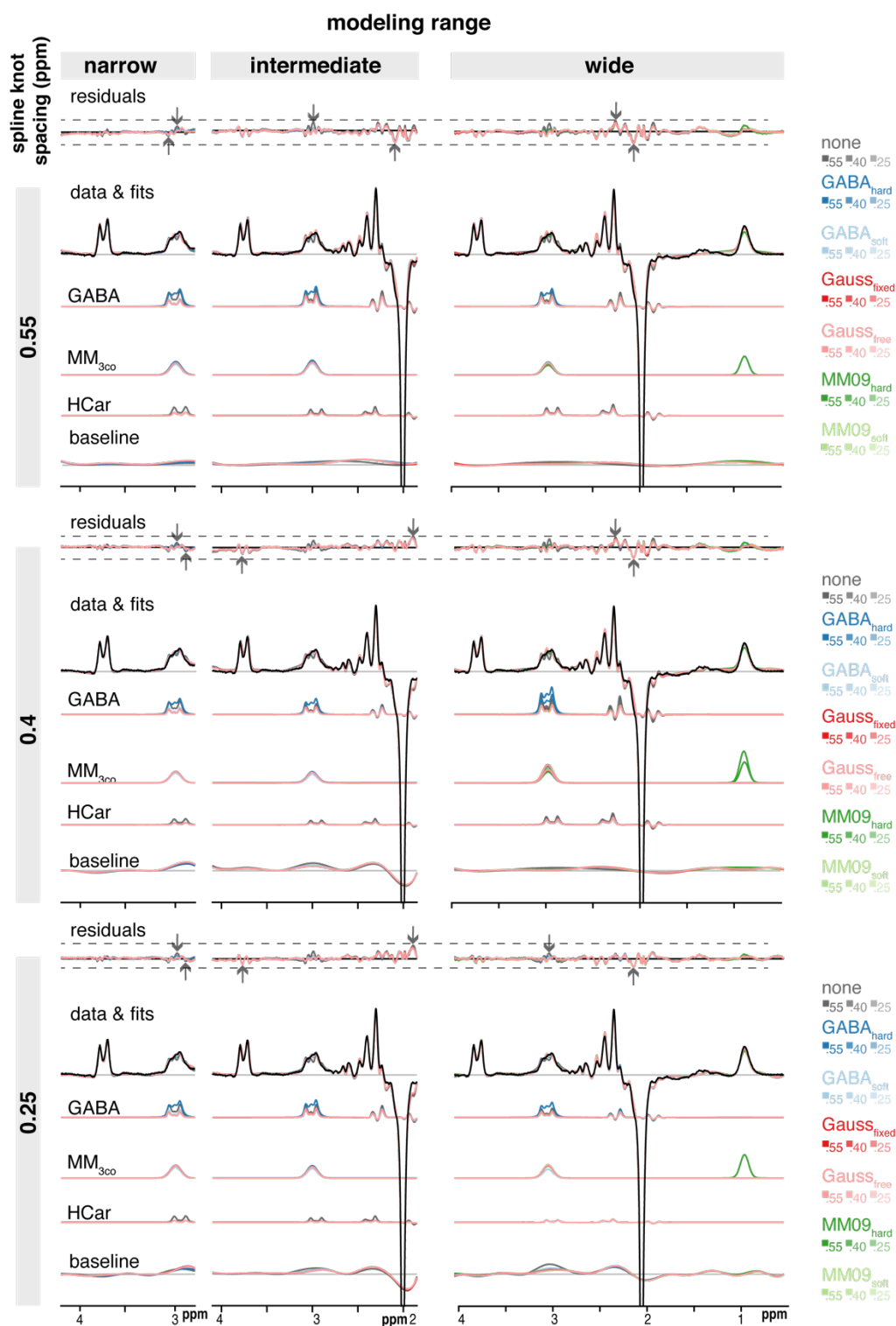
Supplementary Material

Supplementary Material 1 – List of included subjects. All datasets are available at <https://www.nitrc.org/projects/bigga/>

site	subjects	Σ
P01	S01,S02,S03,S04,S06	5
P03	S02,S03,S04,S07,S08,S09,S10,S11,S12	9
P05	S01,S02,S03,S04,S05,S06,S07	7
P06	S01,S02,S03,S04,S05,S06,S07,S08,S09	9
P07	S01,S02,S03,S04,S05,S06,S07,S08,S09,S10,S11,S12	12
P08	S01,S02,S03,S04,S05,S06,S07,S08,S09,S10,S11,S12	12
P09	S02,S03,S04,S07,S09,S10,S11,S12	8
$\Sigma =$ 7		$\Sigma = 62$

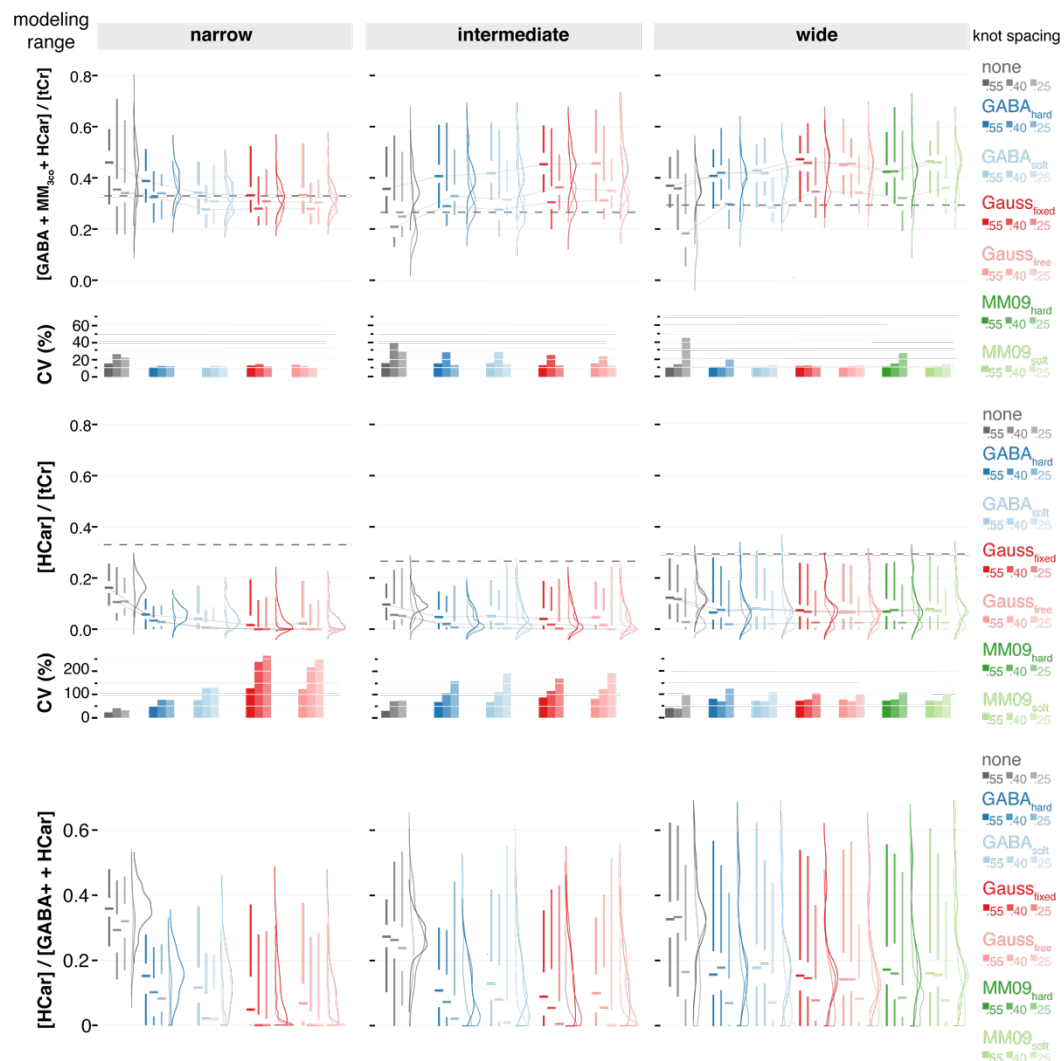
Supplementary Material 2 – GABA+, GABA and MM_{3co} mean and SDs for all modeling strategies (ratios to tCr). Significant differences between the corresponding model and the ‘none’ are indicated in bold. Differences in MM_{3co} are compared between the corresponding model and the GABA_{soft} model.

modeling range		narrow						intermediate		wide	
knot spacing (ppm)		0.55	0.4	0.25	0.55	0.4	0.25	0.55	0.4	0.25	
none	[GABA+]	-	-	-	-	-	-	-	-	-	
	[GABA]	0.22 .062	0.213 .071	0.193 .057	0.297 .048	0.186 .061	0.204 .044	0.284 .029	0.288 .034	0.158 .066	
	[MM _{3co}]	-	-	-	-	-	-	-	-	-	
GAB _{hard}	[GABA+]	0.328 .041	0.291 .04	0.312 .046	0.414 .048	0.296 .062	0.329 .041	0.389 .041	0.414 .047	0.3 .068	
	[GABA]	0.164 .021	0.146 .02	0.156 .023	0.207 .024	0.148 .031	0.165 .021	0.194 .021	0.207 .023	0.15 .034	
	[MM _{3co}]	-	-	-	-	-	-	-	-	-	
GABA _{soft}	[GABA+]	0.298 .029	0.267 .036	0.295 .03	0.417 .053	0.279 .058	0.323 .031	0.375 .039	0.397 .042	0.271 .035	
	[GABA]	0.108 .024	0.102 .027	0.108 .025	0.207 .048	0.13 .039	0.148 .03	0.203 .026	0.204 .027	0.115 .049	
	[MM _{3co}]	0.19 .026	0.165 .025	0.186 .027	0.21 .038	0.148 .033	0.175 .024	0.172 .039	0.194 .032	0.156 .032	
Gauss _{fixed}	[GABA+]	0.306 .04	0.272 .037	0.304 .034	0.412 .052	0.298 .055	0.332 .04	0.369 .05	0.382 .052	0.343 .04	
	[GABA]	0.074 .031	0.08 .031	0.081 .035	0.174 .055	0.106 .045	0.118 .045	0.136 .031	0.145 .032	0.108 .068	
	[MM _{3co}]	0.233 .039	0.192 .038	0.223 .041	0.237 .048	0.192 .03	0.215 .035	0.233 .054	0.237 .045	0.235 .053	
Gauss _{free}	[GABA+]	0.305 .032	0.277 .031	0.3 .035	0.409 .052	0.3 .058	0.331 .04	0.364 .05	0.382 .045	0.341 .043	
	[GABA]	0.079 .034	0.078 .032	0.081 .033	0.18 .054	0.107 .05	0.119 .045	0.137 .033	0.145 .031	0.107 .069	
	[MM _{3co}]	0.226 .038	0.198 .036	0.22 .045	0.229 .044	0.193 .031	0.213 .035	0.227 .057	0.237 .042	0.234 .053	
MM09 _{hard}	[GABA+]	-	-	-	-	-	-	0.396 .039	0.422 .055	0.345 .084	
	[GABA]	-	-	-	-	-	-	0.195 .034	0.189 .032	0.106 .06	
	[MM _{3co}]	-	-	-	-	-	-	0.201 .032	0.232 .043	0.24 .04	
MM09 _{soft}	[GABA+]	-	-	-	-	-	-	0.367 .047	0.386 .045	0.337 .053	
	[GABA]	-	-	-	-	-	-	0.152 .03	0.154 .031	0.098 .072	
	[MM _{3co}]	-	-	-	-	-	-	0.216 .051	0.232 .037	0.24 .045	



Supplementary Material 3 – Mean modeling results and homocarnosine estimates for all modeling strategies with homocarnosine. A substantial structured residual is visible at 3 ppm if for all modeling strategies and for the narrow and intermediate modeling range the homocarnosine concentrations are significantly lower compared to omitting the co-edited MM, especially for knot spacings ≤ 0.4 ppm. All three modeling ranges (columns), three spline knot

spacings (rows), and MM_{3co} model (color-coded) are presented with mean residuals and fits, as well as the GABA, MM_{3co} , homocarnosine (HCar) and spline baseline models. The mean data is included in black. The dashed lines indicate the range of the residual across one row and the arrows indicate the maximum of a specific modeling range and spline knot spacing (color-coded).



Supplementary Material 4 - Distribution of GABA+ plus HCar and HCar estimates and the relative contribution of HCar to GABA+ plus HCar for all modeling strategies. All three modeling ranges (column) and three spline knot spacings (within each column), and MM_{3co} models (color-coded) are presented. Distributions are shown as half-violins (smoothed

distribution), box plots with median, interquartile range, and 25th/75th quartile. CVs are summarized as bar plots.

Declaration of competing interests

The authors have nothing to declare.

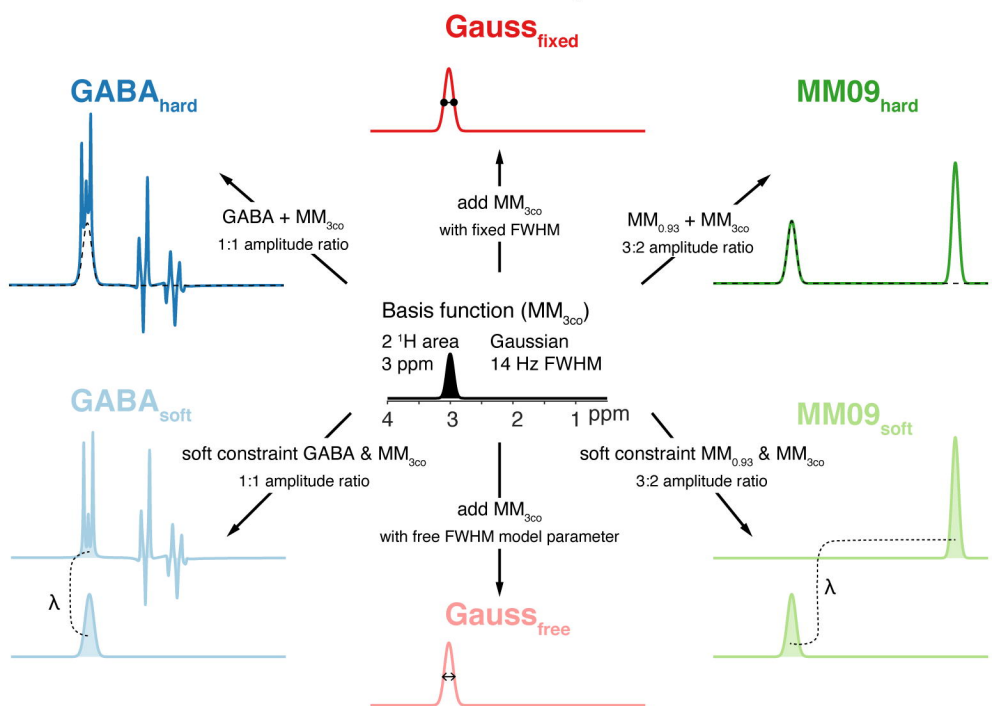
Acknowledgement

This work is supported by NIH grants R01 EB016089, R01 EB023963, R01 EB028259, R21 AG060245, and K99/R00 AG062230.

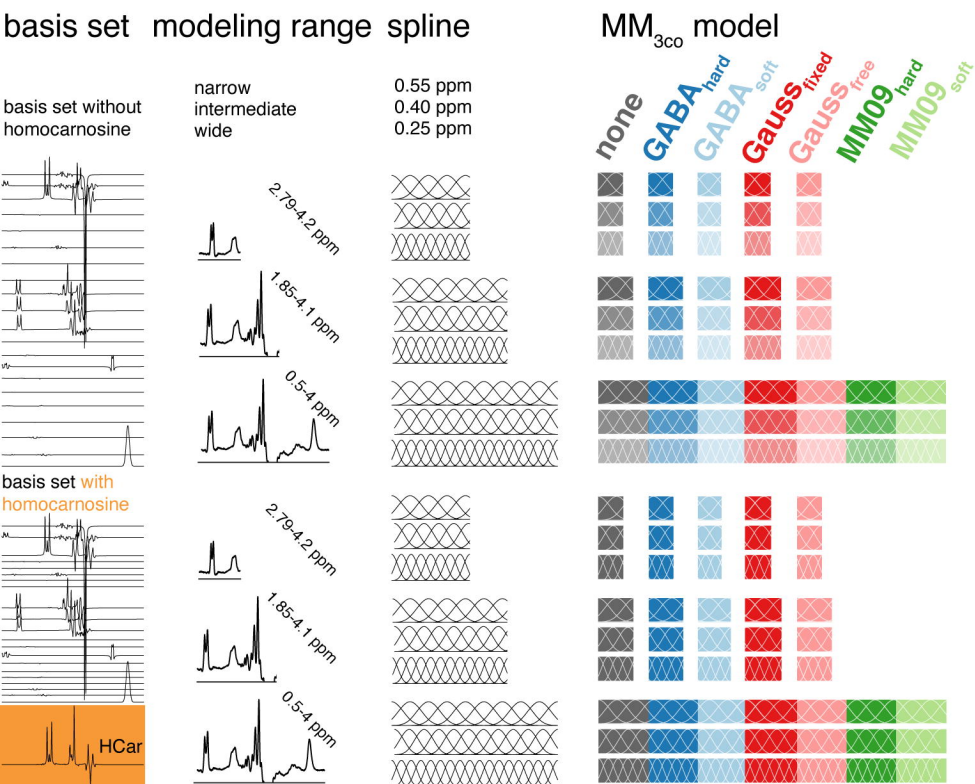
CRediT authorship contribution statement

Helge J. Zöllner: Software, Formal Analysis, Investigation, Writing – Original Draft, Writing – Review & Editing, Visualization. **Sofie Tapper:** Investigation, Writing – Review & Editing. **Steve C. N. Hui:** Investigation, Writing – Review & Editing. **Richard A. E. Edden:** Conceptualization, Formal Analysis, Writing – Review & Editing, Supervision, Project administration, Funding acquisition. **Peter B. Barker:** Writing – Review & Editing, Supervision, Funding acquisition. **Georg Oeltzschner:** Conceptualization, Methodology, Software, Investigation, Formal Analysis, Writing – Review & Editing, Supervision, Funding acquisition.

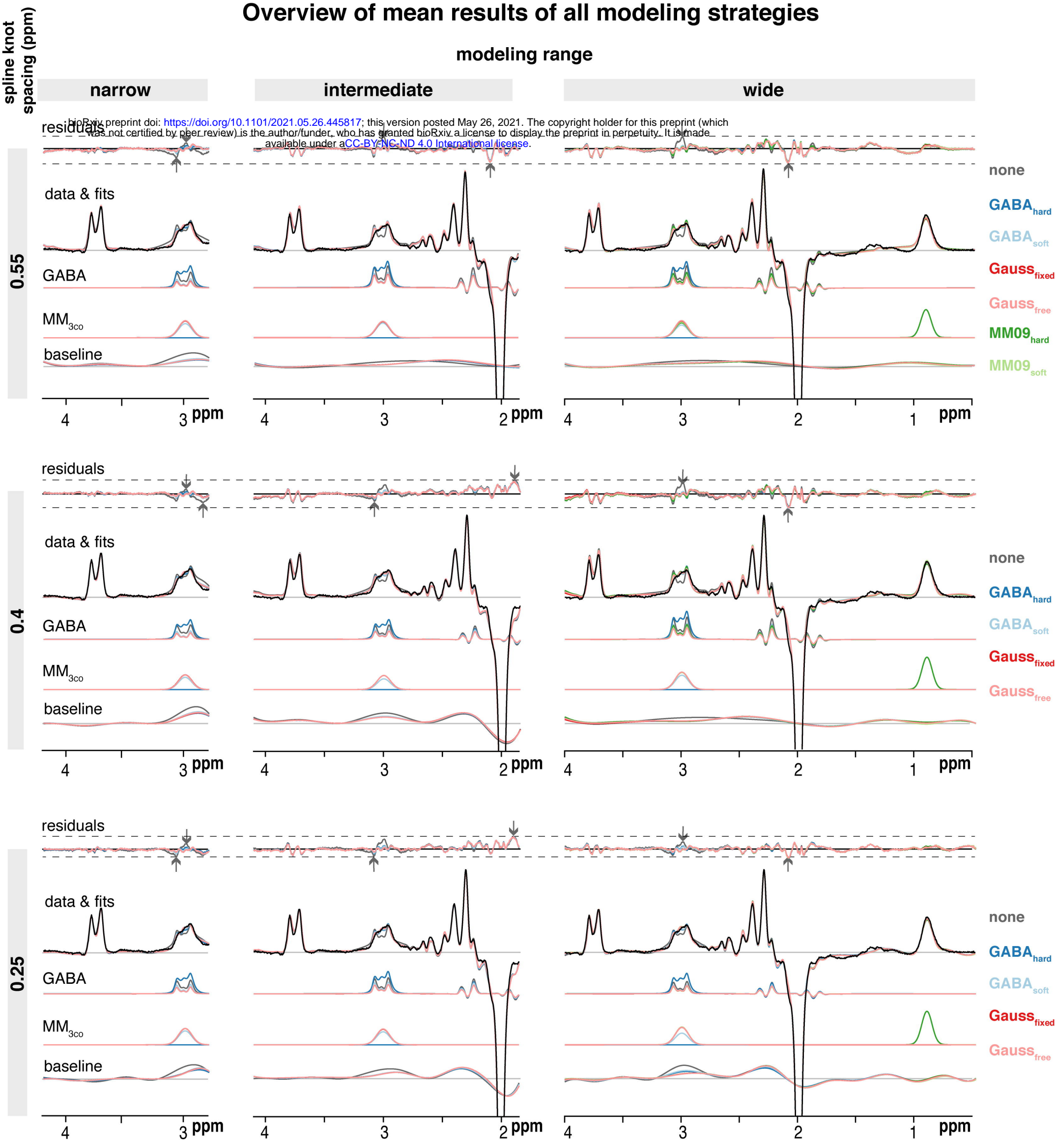
Co-edited MM model implementations



B Combination of modeling strategies



Overview of mean results of all modeling strategies



modeling
range

narrow

intermediate

wide

knot spacing

[GABA + MM_{3co}] / [tCr]

0.6
0.4
0.2
0.0

CV (%)

40
20
0

none

■.55 ■.40 ■.25

GABA_{hard}
■.55 ■.40 ■.25

GABA_{soft}
■.55 ■.40 ■.25

Gauss_{fixed}
■.55 ■.40 ■.25

Gauss_{free}
■.55 ■.40 ■.25

MM09_{hard}
■.55 ■.40 ■.25

MM09_{soft}
■.55 ■.40 ■.25

